

Evaluation of Machining Characteristics and Tool Wear During Drilling of Carbon/Aluminium Laminated

Ali Riza Motorcu

Professor
Çanakkale Onsekiz Mart University
Faculty of Engineering
Turkey

Ergün Ekici

Associate Professor
Çanakkale Onsekiz Mart University
Faculty of Engineering
Turkey

Shivi Kesarwani

Guest Faculty
Madan Mohan Malaviya University of
Technology
Department of Mechanical Engineering
India

Rajesh Kumar Verma

Professor
Harcourt Butler Technical University
Department of Mechanical Engineering
India

In the past few decades, fibre metal laminate (FML) machining has been facing critical challenges in quality control and tool wear monitoring due to the material's intrinsic heterogeneity and abrasiveness. Different drill tools have been used to investigate the effect of process parameters on machining performances. Composite holes and tool wear was studied for drilling forces and surface roughness. An emphasis was made on examining the tool morphologies and wear processes that influence the drilling of CARALL composites. The drilling responses obtained from both the drill bits were optimized using a decision-making approach viz; Combined Compromise Solution Analysis (CoCoSo). The SEM investigation of the machined samples was used to examine the hole quality and surface finish. A lower point angle drill with a longer chip flute length produced the best results for drilling CARALL composites up to a specific point with minimum flank wear and chip adhesion.

Keywords: CARALL, drilling, cutting force, torque, surface roughness, tool wear, CoCoSo.

1. INTRODUCTION

Over the last decade, hybrid composites have been used in various high-performance applications due to their exceptional chemical, physio, and mechanical characteristics. The fibre metal laminate (FML) becomes a suitable candidate to fulfill the varying needs for developing structural components. This is mainly due to their lightweight, durable thermal efficiency and enhanced strength features [1]. FML are the hybrid composites containing alternative thin metal layers and fibre-reinforced epoxy prepregs [2-6]. Fibre metal laminates are materials with high weight savings potential and are highly tolerant damage [7, 8]. Among the current FML, the best-known examples are aramid-reinforced aluminium laminates (ARALL) with aramid fibres, glass fibre/aluminium reinforced epoxy (GLARE) with glass fibres, and carbon-reinforced aluminium laminates (CARALL) with carbon fibres [5, 9-10]. During the manufacturing and assembly of aircraft parts, different holes are required to develop the final product for riveted and bolted connections [11]. While up to 300,000 holes are required in a jet fighter, the number of holes required by a commercial aircraft ranges from 1.5 to 3 million [12]. Poor hole quality when drilling fibre-reinforced composite leads to the rejection of 60% of all parts in the assembly phase [13]. Close dimensional and geometric tolerances have been followed in processing polymeric composite materials, but it has yet to be very successful due to the nature of

polymeric materials [14-16]. In addition, due to the different mechanical properties and machinability aspects of fibre and metallic materials, FML machining becomes a complex task for the manufacturing sector [17]. As a result, stress and strain are generated at different rates in FML composites, which creates a difference in elastic modulus between the composite and the metal. There is a chance of circularity error in generated hole diameters, which can lead to assembly failures. There is an extreme need to explore the machining aspect of FML composites in society and trade interests. Eminent scholars use different reinforcing materials to enhance the metal matrix properties. Giasin and Ayvar-Soberanis investigated the drilling aspect of GLARE composites and examined the formation of burr, chip morphology, and delamination causes using variance analysis. A decrease in hole size was observed at the exit with increasing cutting speed and decreasing feed rate [18]. Pawar et al. investigated the hole quality in drilling GLARE laminates with tools of different geometries. Due to the different elastic modulus and coefficient of thermal expansion of the drill and workpiece materials, all four drills produced slightly smaller holes during the GLARE drilling process [19]. Park et al. use varied drilling constraints to examine the drilled hole quality and delamination generated in GLARE composite samples. The findings reveal that the effect of feed rate and tool hardness is the most significant factor for drilling-induced damages in GLARE samples. This work recommends combining high cutting speed and low feed values for quality machined surfaces. The higher bending of the workpiece plays an important role, and it could be regulated using a backing plate. Without this, the hole perpendicularity error can cause more on thinner laminates [20]. Temperature causes

Received: March 2024, Accepted: May 2024
Correspondence to: Prof. Dr. Ali Riza Motorcu
Çanakkale Onsekiz Mart University, Faculty of Engineering, Terzioğlu Campus, 17100-Çanakkale, Turkey.
E-mail: armotorcu@comu.edu.tr
doi: 10.5937/fme2403343M

© Faculty of Mechanical Engineering, Belgrade. All rights reserved

FME Transactions (2024) 52, 343-359 **343**

thermal degradation and affects the hole perpendicularity of the laminated composites [21]. Giasin et al. reported that when drilling unidirectional GLARE fibre metal laminates, cutting speed and feed rate significantly affect cutting forces, fibre orientation has no effect on cutting forces, and fibre orientation only affects surface roughness [22]. Giasin et al. remarked that the highest average roughness and mean roughness depth values were obtained with TiAlN-coated and the lowest TiN-coated tools. Lower feed rates and cutting speeds have been found to produce better hole roughness regardless of the cutting tool coating used [23]. Ekici et al. explore the machinability of CARALL samples during drilling operations. The coated and uncoated twist drills with a 6 mm diameter were used as cutting tools in drilling tests. The machining characteristics were analysed using a Grey-Principal Component Analysis (PCA) hybrid optimization tool. The drilling constraints were explored to achieve the optimal response value of thrust, surface roughness, and delamination factor [24]. Also, Ekici et al. examined the cutting tool coating properties for quality hole generation using the drilling of CARALL laminate samples. The findings remarked that the higher feed provides the nominal hole diameter value for the hole's top and bottom surfaces. The efficient results were obtained by uncoated tools, followed by the TiN-TiAlN-coated and TiAl/TiAlSiMoCr-coated carbide drills [25].

From the exhaustive literature survey, it is remarked that the primary focus was made by scholars on drilling multilayer FML composites. However, there is an extreme need to explore the machinability aspect and control parameters to achieve the desired response value and efficient machining environment. The work related to GLARE, ARALL, and carbon-fibre reinforced polymer (CFRP) /Ti stack composites was explored by analysing the effects of various drilling techniques and parametric responses. However, there needs to be more research in the scientific literature on the concerns of finding parametric impacts on various drilling responses, particularly drilling forces and hole quality. The effect of different tool performances and disclosing the tool wear modes influencing the CARALL composite. The work related to the machining exploration of CARALL is passing through a transition phase. Still, its higher mechanical properties and chemical aspects are improved than other metal composites. The drilling of CARALL is highly required to generate a quality machined surface free from defects and machining-induced damage. It is possible to control the drilling parameters using a robust optimization tool. A recently developed optimization tool for the Combined Compromise Solution Analysis (CoCoSo) module is proposed in the current work to identify the optimal process parameter. The obtained finding can offer the desired value of quality and productivity indices during the machining of CARALL samples using different geometry cutting tools. During the drilling process of CARALL composites, the surface roughness (S_a) and cutting forces concerning the tool shape, cutting speed, and feed rate were examined. CARALL

composites were tested using high-strength CFRP laminates and Al 5754 alloy with two different twist drills. This research is significant because it identifies the feasibility of employing several specialty drills to increase the machinability of the CARALL composite. Drilling forces, surface morphologies of drilled holes, and tool wear resulting from varied cutting parameters were used to evaluate surface finish, structural integrity, and wear characteristics of composite with different drill bits. This study compares the performance of two tool geometries, one in fibre-reinforced polymer composites and the other in drilling metallic stack materials, whose performances have been revealed by scientific studies in drilling CARALL composites. The tool geometry results investigated under the specified cutting conditions will provide valuable information to the literature on developing tool geometries for drilling fibre metal laminate composites.

This study is one of the pioneering studies in the literature examining CARALL composites' machinability. It is one of the rare studies on CARALL that includes statistical analyses and experimental evaluations. This eliminates likely the lack of research on tool geometry in the literature and the lack of statistical significance of experimental data. The results presented in this work will add to the corpus of knowledge in CARALL composite machining and help researchers know the relationships between process parameters and drilling reactions that can help steer composite applications in industries like the automotive and aerospace sectors.

2. MATERIALS AND METHOD

A metal alloy (Al5754) and a carbon-fibre reinforced polymer (CFRP) composite constitute the CARALL composite. Three layers of 245 g/m² woven prepreg carbon fibre are constructed for each CFRP plate. CARALL composite structure consists of 3 layers of aluminium (Al5754), each 0.5 mm thick, and 4 CFRP layers, each 0.9 mm thick. All CARALL samples are equal in thickness (~5.1 mm) (Figure 1). This study used mechanical abrading of Al 5754 alloy with 400 grit sandpaper and subsequent rinsing with clean water to improve contact characteristics between carbon fibre and aluminium. Before anodizing, the samples were etched with alkali for 6 minutes at 60 °C in 100 g/L sodium hydroxide (NaOH) electrolytes and washed with distilled water to remove any remaining alkali. The sample was maintained at room temperature in 200 mL/L nitric acid (HNO₃) for the next four minutes, and then distilled water was used to rinse it. An anodizing took 15 minutes in an electrolyte containing 180 g/L sulphuric acids. CARALL synthesis began immediately after this treatment was completed since the Al plates were enclosed in vacuum bags (in less than 60 min). As illustrated in Figure 1, CARALL samples with dimensions of 500x500 mm were prepared in seven layers, including four carbon fibre layers and three Al layers, and then cured at 125 °C for one hour under a compressive force of 15 tons.

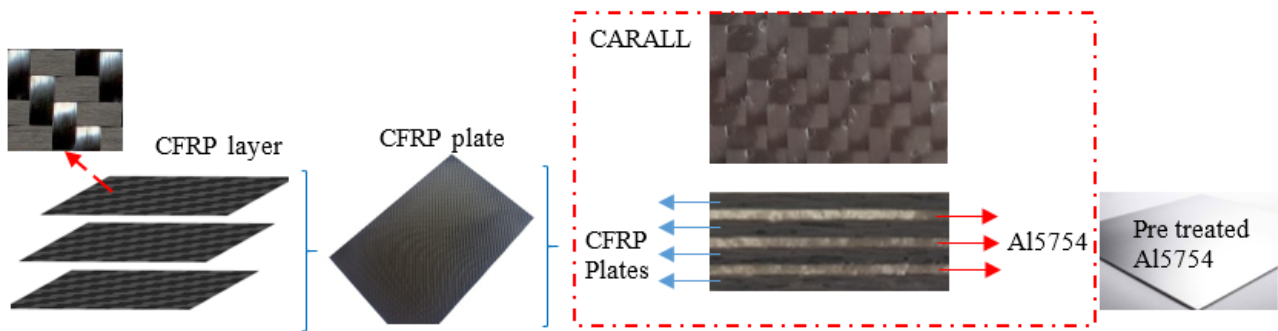


Figure 1. Production of CARALL samples.

2.1 Machinability experiments

To conduct the drilling experiments, the CARALL material was fabricated, and the trial workpieces of 110 x 80 mm were cut using a water jet. Under dry-cutting circumstances, drill trials were performed in a Johnford VMC850 vertical machining centre. Two different drills with special (Tool 1) and standard (Tool 2) geometry, supplied by Sandvik Coromant company and whose technical and geometric features are shown in Figure 2, were used in the drilling experiments. The most commonly used diameter in the aviation industry, 6.35

mm, was preferred in the experiments conducted under dry drilling conditions.

Table 1 depicts the tool geometry and nomenclature. Cutting speed (V_c), feed rate (f), and cutting tool ($Tool$) were considered three process variables (Table 2). Drilling experiments with both tools are carried out separately using the experimental design (DoE) approach known as Taguchi L18 orthogonal array (OA) (Table 3).

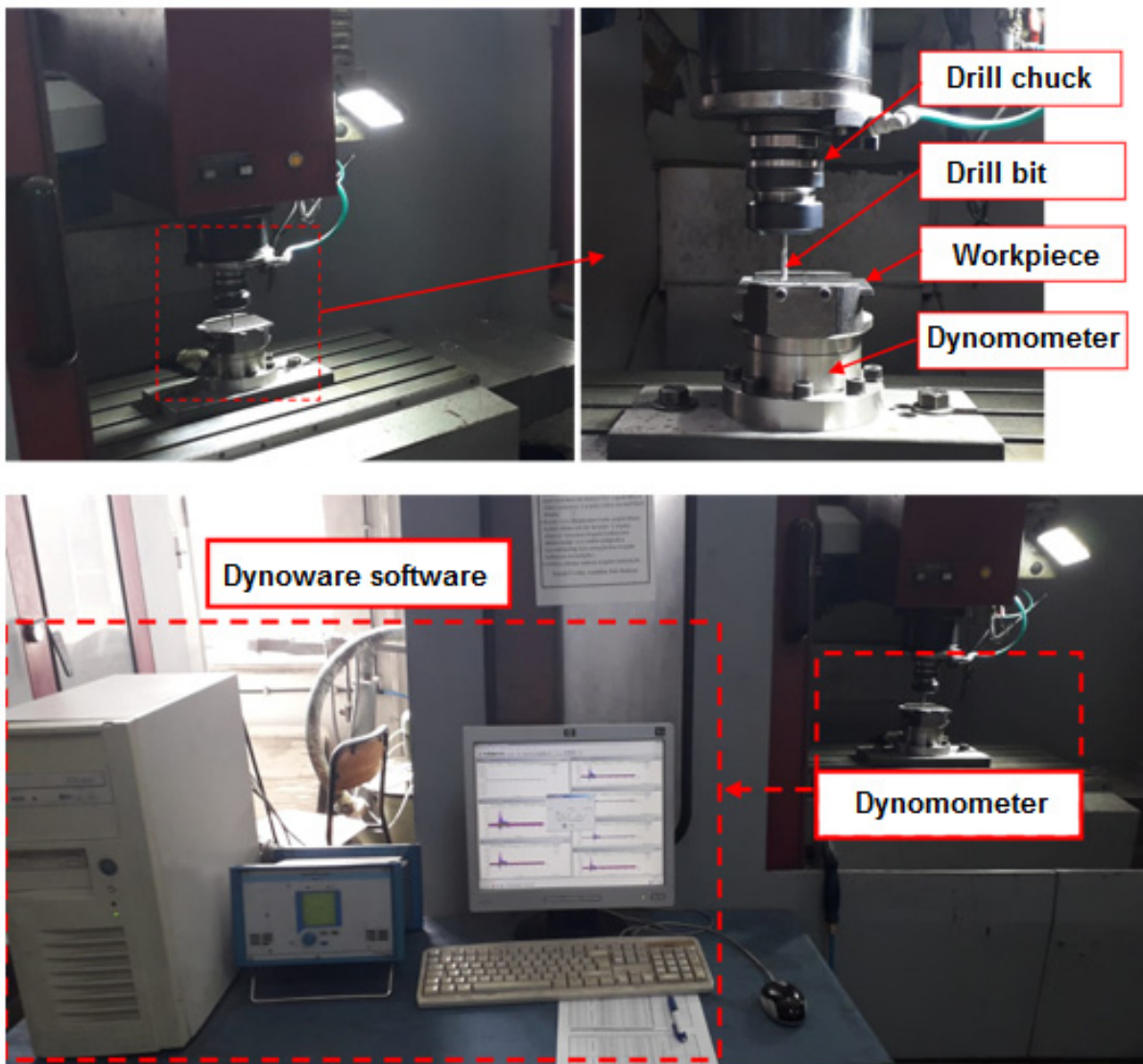


Figure 2. Experimental setup for the drilling of CARALL composite.

Table 1. Geometry and technical features of cutting tools.

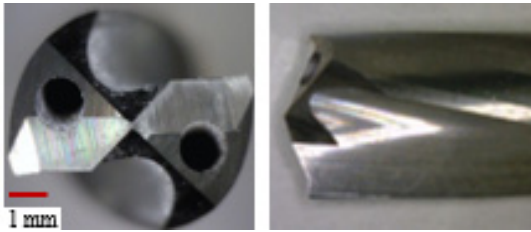
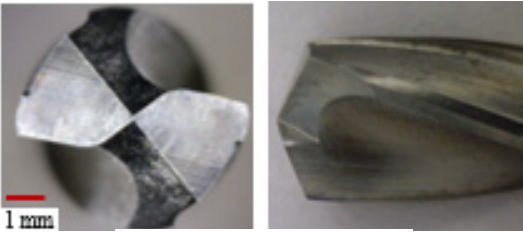
Tool type	Tool 1	Tool 2
Tool code and geometry	 (860.1-0635-051A1-NM H10F)	 (452.1-0635-044A0-CM H10F)
Grade	H10F	H10F
Cutting diameter	6.35	6.35
Point angle	130°	135°
Usable length	51.7	44.45
Chip flute length	80	50.8
Point length	0.9	1.316
Functional length	120.1	100.3
Functional length	121	101.6

Table 2. Levels of process variables.

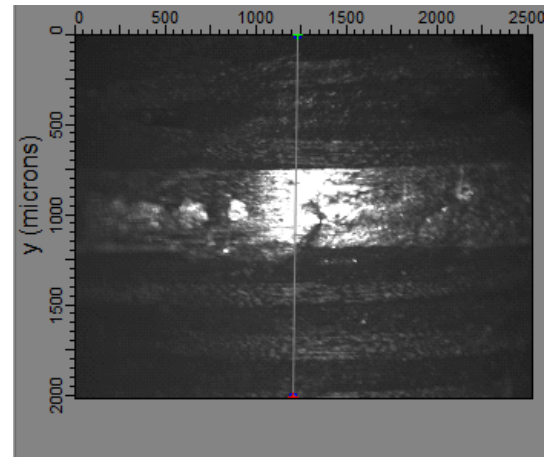
Levels	Cutting Speed (m/min)	Feed rate (mm/rev)	Cutting Tool
	V_c	f	$Tool$
1	70	0.08	Tool 1
2	91	0.112	Tool 2
3	118	0.156	-

Table 3. Taguchi design and corresponding experimental data for both tools.

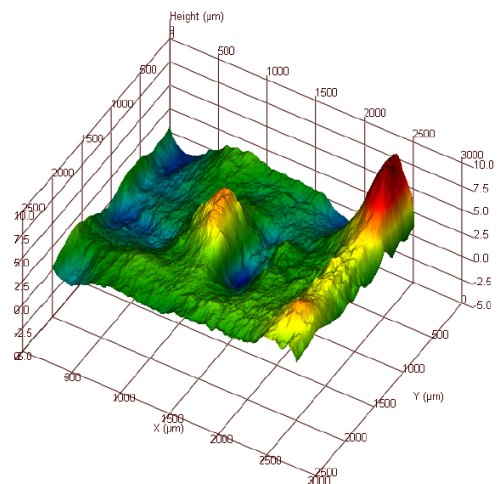
Tool	Exp. No.	V_c	f	S_a (μm)	F_z (N)	T (N.cm)
T1 (860.1 NM H10F)	1	70	0.08	0.880	98.18	43.16
	2	70	0.112	0.840	131.56	45.68
	3	70	0.156	0.752	142.85	49.07
	4	91	0.08	0.894	97.745	38.50
	5	91	0.112	0.965	125.00	42.48
	6	91	0.156	0.984	140.73	46.34
	7	118	0.08	0.997	98.57	42.58
	8	118	0.112	1.008	122.16	39.12
	9	118	0.156	0.972	136.83	44.35
T2 (452.1 CM H10F)	1	70	0.08	1.254	88.855	32.69
	2	70	0.112	3.667	112.78	39.62
	3	70	0.156	2.242	139.92	46.85
	4	91	0.08	2.931	84.405	31.34
	5	91	0.112	3.414	110.45	35.99
	6	91	0.156	4.119	132.05	38.32
	7	118	0.08	3.262	85.91	28.64
	8	118	0.112	3.812	108.97	37.41
	9	118	0.156	3.440	127.52	37.89

2.2 Drilling response

Thrust force and torque measurements were performed on a Kistler 9272 dynamometer with Dynaware software. Phase View ZeeScope optical profilometer evaluated 3D surface roughness along the hole axis to cover 2 CFRP and 1 Al layer (Figure 3. a) and captured 3D surface pictures to execute the measurements precisely. The samples had been cut perpendicular to the hole axis (Figure 3. b).



(a)



(b)

Figure 3. (a) Surface roughness measurement direction, (b) Sample 3D isometric views of surfaces.

2.3 Combined Compromise Solution Analysis (CoCoSo) technique

When more than two responses are considered to be evaluated concurrently, CoCoSo ensures that two or more conflicting parameters are consistently optimized within specific constraints. In this scholarly article, all

responses to the machining parameters are rated as "lower is better," with the smallest being the best. Equal weight priority has been utilized in this technique since various earlier researchers had already incorporated it during the assessment of similar multiple-criteria decision-making (MCDM) methodology. The following procedures were used to assess the efficacy of the CoCoSo approach:

Step 1: Initially, development of the decision matrix (DM).

$$E_{ij} = \begin{bmatrix} e_{11} & e_{12} & \dots & e_{1n} \\ e_{21} & \dots & \dots & e_{2n} \\ \dots & \dots & \dots & \dots \\ e_{m1} & e_{m2} & \dots & e_{mn} \end{bmatrix}; i \in [1, m], j \in [1, n] \quad (1)$$

Step 2: DM Normalization based on the benefit as well as cost criteria.

$$C_{ij}^k = \frac{e_{ij} - \min e_{ij}}{\max e_{ij} - \min e_{ij}} \quad \text{Benefit Criterion} \quad (2)$$

$$C_{ij}^k = \frac{\min e_{ij} - d_{ij}}{\max d_{ij} - \min d_{ij}} \quad \text{Cost Criterion} \quad (3)$$

Step 3: If several alternatives have varying attributes, the weighted comparability (w_i) sequence and the entire power weight of comparability sequences for each alternative are utilized to find an average weighted combination. The equations below are used for each alternative to summate the weighted normalized matrix (S_i) and the power weights (P_i) of comparability sequences.

$$S_i = \sum_{j=1}^n (w_i^0 C_{ij}^k) \quad (4)$$

$$P_i = \sum_{j=1}^n (C_{ij}^k)^{w_i^p} \quad (5)$$

Step 4: In CoCoSo, the relative weight of estimated strategies is determined by applying one of three different aggregation procedures. These relative weights are generated based on the following equations.

$$H_{ci} = \frac{P_i + S_i}{\sum (P_i + S_i)} \quad (6)$$

$$L_{ci} = \frac{S_i}{\min S_i} + \frac{P_i}{\min P_i} \quad (7)$$

$$M_{ci} = \frac{\lambda S_i + (1 - \lambda) P_i}{\lambda \max S_i + (1 - \lambda) (\max P_i)} \quad (8)$$

Step 5: The equation that is used to get the conclusive ranking order of the options that were examined in line with the CoCoSo technique is as follows:

$$K_{ci} = (H_{ci} \times L_{ci} \times M_{ci})^{\frac{1}{3}} + \frac{1}{3} (H_{ci} + L_{ci} + M_{ci}) \quad (9)$$

3. RESULTS AND DISCUSSIONS

3.1 Analysis of the cutting forces

In order to understand the drilling mechanism of CARALL composite, it is necessary to investigate cutting

forces. Cutting forces may reveal a great deal about the quality of holes and the wear of the drills; thus, it is essential to investigate the mechanism and effect of cutting force. Figure 4 depicts the thrust forces (F_z) signals in the time domain concerning different drill bits for the scenario corresponding to 70 m/min and 0.08 mm/rev, respectively. Also, the thrust force is a broad term that refers to tribological engagements at the tool-work interface that occur toward the feed direction. It is an essential parameter in determining the scope of interfacial deformation. In the stable cutting zone, except for the hole entry and exit sides, high fluctuations in thrust force signals are observed, which can be attributed to the cyclic chip separation process of the CARALL composite and the dynamic widely differing chip removal mechanisms caused by the variation of material layers from CFRP and Al. Also noteworthy is that the Tool 1 drill bit provides the lowest orders of magnitude of thrust forces among the drills tested. Its lower point angle and higher chip flute length reduce point forces and improve chip separation during machining CARALL composite. Furthermore, the Tool 1 and Tool 2 drill bits display identical fluctuations in thrust force signals as a function of the time spent drilling. As the drill approaches the workpiece (see Phase 1 in Figure 4), the chisel edge makes contact with the composite, causing a quick rise in thrust force due to the rubbing and plowing actions on the composite.

Furthermore, when both the drill bit and the Al sheets in the CARALL composite come into contact with each other, the thrust force values increase rapidly but at a much slower rate than with the twist drill, which is due to the functionally designed drill tip structure that favours the minimization of drilling forces. As a result, Phases 2, 4, and 6 for both drills occur, during which a steady rise in thrust force is observed as the cutting lips come into contact with and the chisel edge pierces the CFRP layer. The maximum magnitudes of thrust forces are also obtained for both drills when the chisel edges pierce the Al layers, as demonstrated in Phases 3, 5, and 7, respectively. The change in thrust force in the entrance regions demonstrates the impact of the drill tip angles on the drilling forces in the entry regions of the holes [26-27]. It was evident that the thrust force varied dramatically during Phase 1 but only slowly increased during Phase 2 due to the shift in the point angle of the drill lips. In phase 5, the highest thrust force is observed when both drill bit lips fully engage in the workpiece. This is also the phase in which the danger of inter-laminar delamination is predicted to be higher, as the chisel edge drives out the last plies of materials. Once the drill lips have emerged from the hole and the flutes have entered the workpiece after going through Phase 8, the amplitudes of the thrust force begin to decrease significantly. Drilling is completed in step 8, and the reaming process commences, with the drill bit being used to ream out the hole to its final size. Due to the lesser stiffness of the drill/workpiece combination, reaming is more prone to vibrations and chattering than drilling, which could also affect the resulting hole size and quality. The thrust force is an important indicator for evaluating machinability properties and power consumption [27].

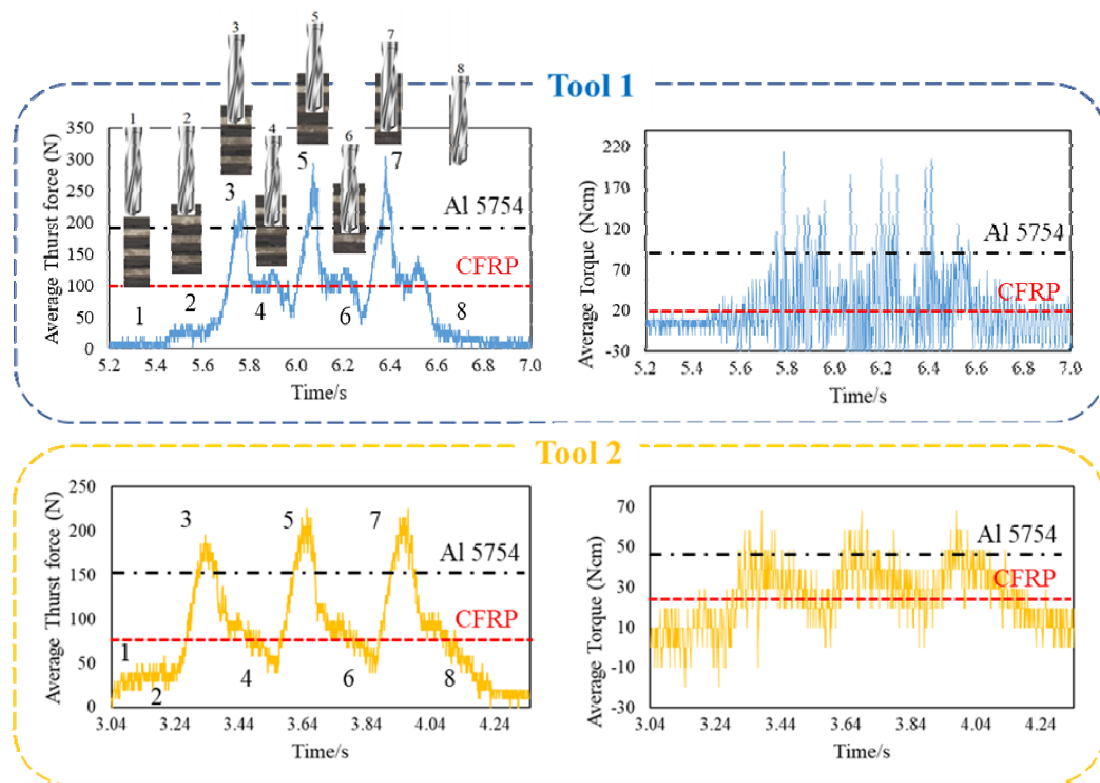


Figure 4. Characteristic phases in time series of thrust force and torque in drilling experiments.

Using high-strength CARALL composite for machining, Figures 5 and 6 display the impact of drilling settings on the magnitudes of average thrust forces (F_z) and average torque (T) for each drill bit. The increased feed rate shows a noticeable rise in the average thrust force for both drills. The average thrust forces in both tools in CARALL drilling increase with increasing feed rate, as shown in Figure 5. Because of the increased cross-section of chips produced while drilling CARALL composites, a consistent incremental phenomenon can be observed between the average thrust force and the feed rate, which could be seen for both drills during the investigation. When the feed rate was increased from 0.08 mm/rev to 0.156 mm/rev at a constant cutting speed of 70 m/min, the average thrust force increased by 45.52 percent and 57.47 percent for Tool 1 and Tool 2, respectively (Table 3). With increasing feed, larger uncut chip thicknesses and higher cutting energy

consumption requirements necessitate the drill bit to cut a larger volume of material per revolution and overcome much higher cutting resistance [28]. Average thrust forces for both tools decrease as cutting speed increases (Figure 5). When the feed rate was increased from 0.08 mm/rev to 0.156 mm/rev at a constant cutting speed of 118 m/min, the average thrust force increased 38.82 percent and 48.44 percent for Tool 1 and Tool 2, respectively. This demonstrates that as the cutting speed increased from 70m/min to 118m/min, the average thrust forces decreased by 6.7 and 9 % for Tool 1 and 2, depending on the feed rate change. Similarly, Zitoun et al. [29] reported that cutting speed reduced thrust force (Al approximately 5%, CFRP approximately 10%) when drilling CFRP/ Aluminium (Al) sandwich composites with uncoated drills at a constant feed rate (0.15 mm/rev).

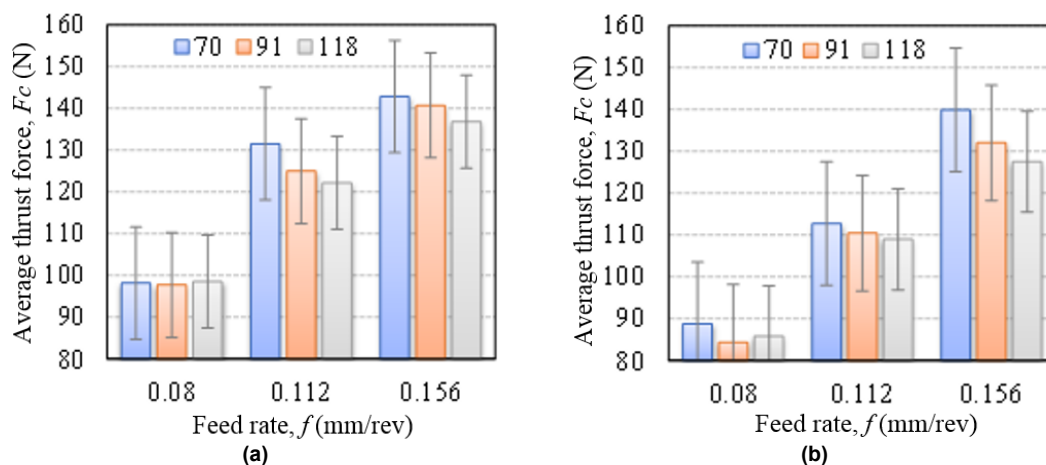


Figure 5. Average thrust force (F_z) in function of f and V_c : (a) Tool 1, (b) Tool 2.

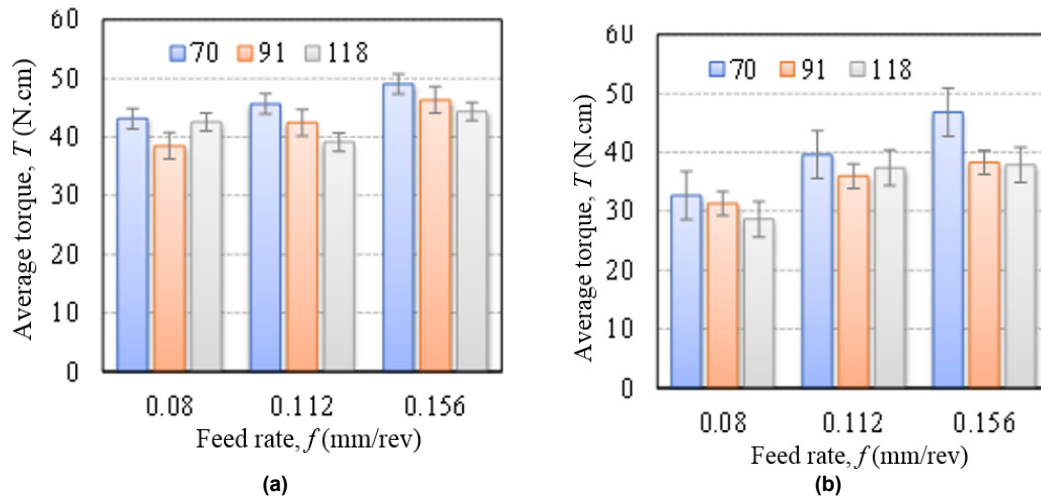


Figure 6. Average torque (T) in function of f and V_c : (a) Tool 1, (b) Tool 2.

According to Koplev et al. [30], increasing cutting speed had two effects: reducing thrust force and increasing drilling temperature. While increasing the cutting speed raised the temperatures in the cutting zone and aided plastic deformation of the aluminium (Al) sheets, it decreased average thrust forces due to softened epoxy in CFRP [24]. Compared to Tool 1, Tool 2 provided a 2.09 percent -16.64 percent reduction in average thrust forces. In the study by Xu et al. [31], brad spur drills produced higher thrust forces in all drilling conditions than twist drills when drilling high-strength CFRP composite. This is due to the additional thrust created by Tool 1's outer corner end structure compared to Tool 2's straight main cutting edge line. When drilling CARALL, feed rate has a much greater impact on average thrust forces than tool geometry and cutting speed. As a result, a low feed rate and high cutting speed can be recommended for twist drills to reduce average thrust force. Torque values increased by 20.33% and 43.31 %, respectively, as the feed rate increased for Tools 1 and 2 (Figure 6 and Table 3). On the other hand, torque values decreased by 10.64 and 23.64%, respectively, as cutting speed increased for Tools 1 and 2 (Figure 6, Table 2). Similarly, many researchers have presented in the literature [28-35] torque results that increase feed rate and decrease cutting speed when drilling FML and fibre-reinforced composites. While Tool 1's average torque was 42.58 Ncm, Tool 2's average was 28.64 Ncm, obtained with Tool 2, which has a higher tip and helix angle (Table 3). Average torque values decreased from 4.57%-48.67% with Tool 2 compared to Tool 1. This increase in torque values parallel to the average thrust force (F_z) in Tool 1 compared to Tool 2 can be attributed to Tool 1's two protruding outer edge geometries. The literature has presented that two geometric angles, the tip and helix angles, affect the torque ratio in the nominal force generation [36, 37].

3.2 Analysis of the surface roughness of machined surface

Figure 7 summarizes the surface roughness testing on the holes at various feed rates. It illustrates that the drilling parameters such as geometry, feed rate, and

cutting speed affect the measured surface roughness of the drilled hole. The findings of the surface roughness graphs reveal that the values obtained for Tool 1 (between 0.752 and 1.008 μm) are lower than those produced for Tool 2 (between 1.254 and 4.119 μm) for both geometries. Chip removal should be made easier by the flute shape of a drill bit with a suitable geometry for the surface quality of the hole being drilled. This prevents chips from damaging the hole's surface, ensuring no damage occurs. Because of its flute design, Tool 1 may be concluded to optimize chip flow during drilling and improve hole quality by reducing chip clogging while the tool is in use. Cutting speed positively correlates with average surface roughness, while feed rate negatively correlates with average surface roughness.

As detailed in the literature, this is a comparable situation. The surface quality of a cut can be improved by increasing the cutting speed to a particular threshold.

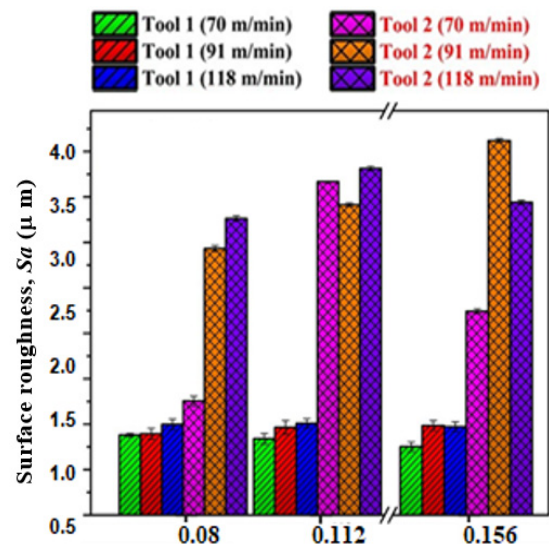


Figure 7. Comparison of surface roughness attained via different drills.

The surface obtained during the drilling of the CARALL composite by both the drill bits is evaluated, and the 3D topology views for maximum and lowest surface roughness are described in Figure 8. As a result, it has been established that the surface contour derived

from Tool 1 is more uniform and homogenous when compared to the surface contour determined from Tool 2. In the experiments, it was encountered that the surface roughness of the drilled hole at a feed rate of 0.112 mm/rev was higher than the surface roughness at a feed rate of 0.08 mm/rev for both tools. Furthermore, using a Drill bit with a 130°-point angle, the results revealed that the qualities of the drilled hole surface finishing improved appreciably at a lower cutting speed, which was previously unknown. The surface roughness value of the hole drilled with Tool 2 is greater than that of the hole drilled with Tool 1. Overall, the surface roughness value rose straight-forwardly with increasing feed rate for both tools.

The image of cross-sectioned holes taken with a Scanning Electron Microscope (SEM) is shown in Figure 9. The most severe damage occurred at the

greatest feed rate (0.156 mm/rev) on various stacked plate layers. A fibre detachment, edge widening, and micro cracks on the CFRP entrance edge were discovered, caused by tool pressure and sharp metal chips rubbing on the edge of the CFRP lamination [38, 39]. Al laminates were used to safeguard the areas between CFRP layers and the CFRP exit, which were less prone to damage. Since metal chips were evacuated through CFRP, it is apparent that the damages on the initial CFRP hole wall and between CFRP laminates were more severe than those on the exit CFRP. This was due to the rough surfaces caused by metal chip evacuation through CFRP [40, 41]. The final CFRP laminate exit edges were more sensitive to protrusions on the edges and cracking due to the drill's push-out impact; nevertheless, fibre detaching was also seen on this side of the laminate [28, 42].

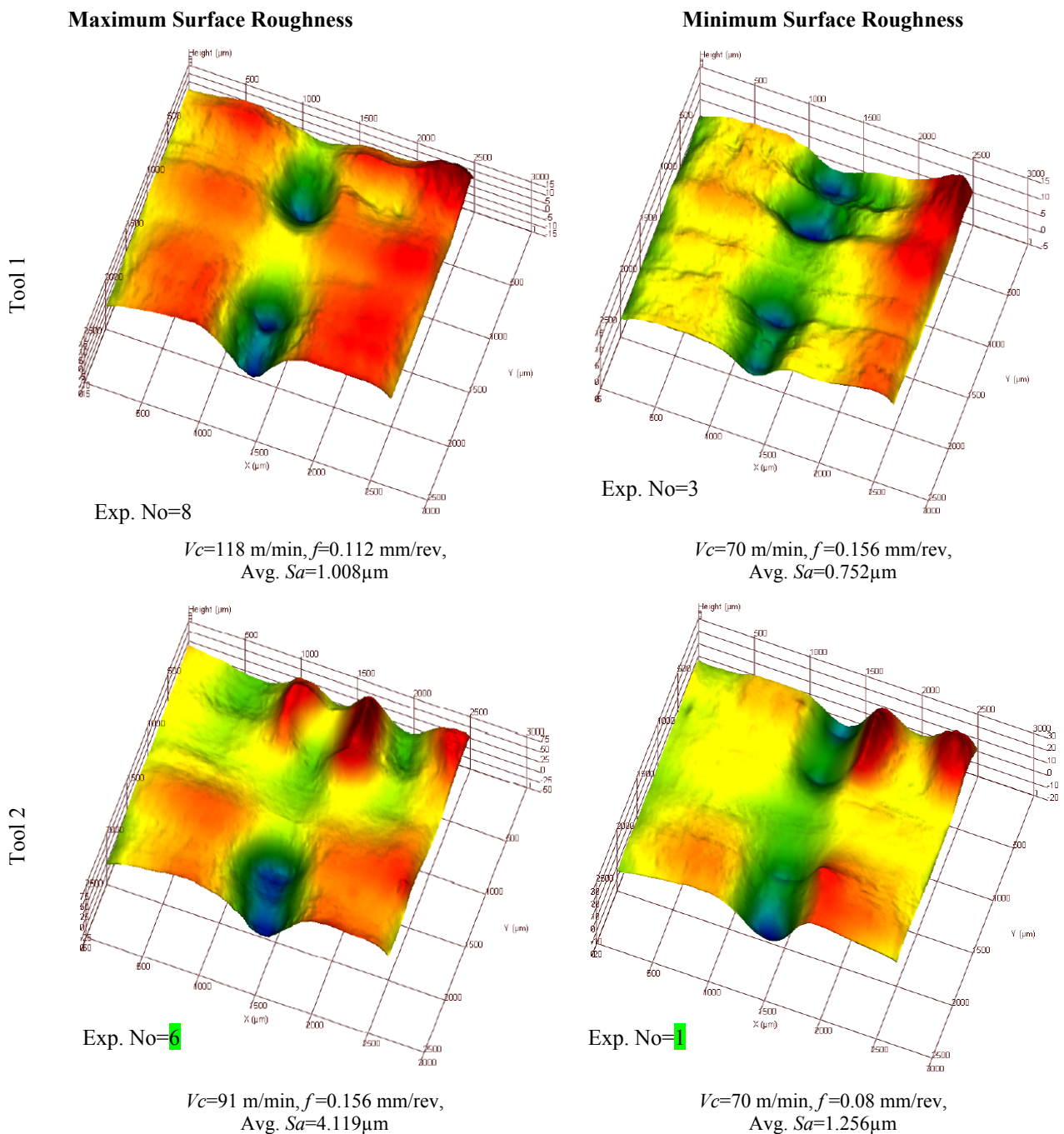


Figure 8. 3D topology views of hole surfaces machined with different drills.

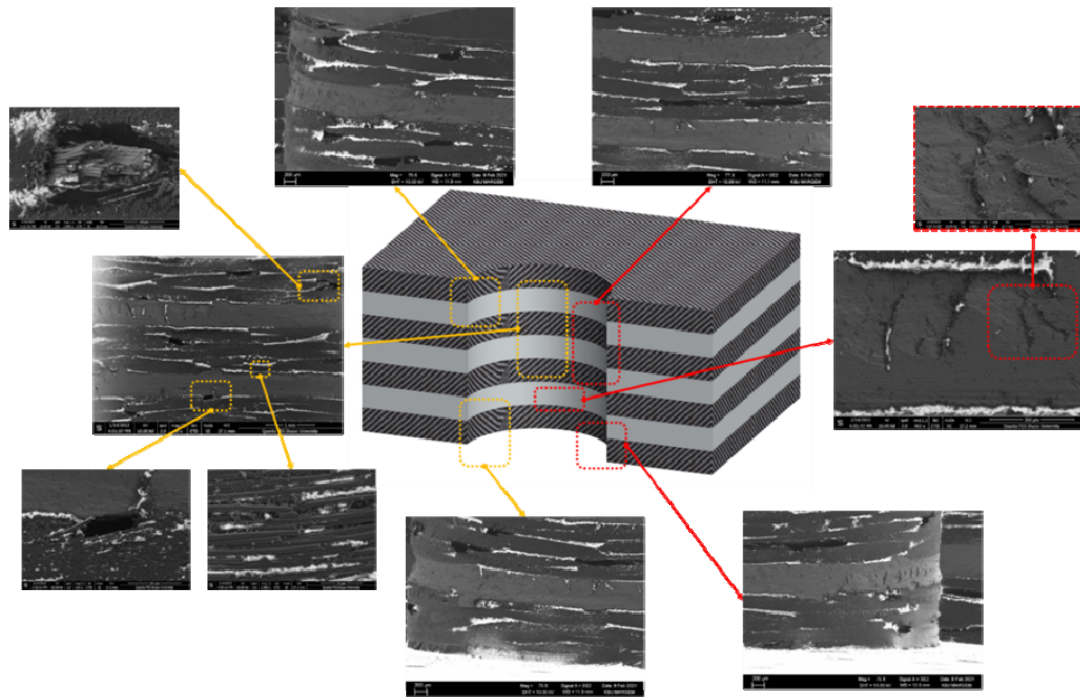


Figure 9. SEM morphology of drilled hole surface.

3.3 Tool wear analysis

The machining of fibre-based composites leads to rapid tool wear progression and limited tool life due to the abrasive behaviour of fibres. The findings of previous works remarked that the abrasive wear leads to the aggressive cutting-edge rounding and fracture/chipping of drill edges during the machining of carbon-fibre reinforced polymer (CFRP) composites [28, 38-42]. The drilling of composite laminates generates different types of machining, which induce damage on the surface of the workpiece and tool body. The Scanning Electron Microscope (SEM) investigations of worn drill surfaces

were conducted to establish the key wear mechanisms and potential failure.

These findings were reported in an in-depth study in Figures 10 and 11, which show worn tool surfaces taken after six holes had been drilled with cutting speeds and feed rates of 118 m/min and 0.156 mm/rev, respectively. Tool 1 has very little edge rounding due to the lower point angle and larger chip flute length, which help alleviate the strong rubbing impacts of the reinforcing fibres on the tool. SEM inspection also reveals the amount to which powdered carbon adheres to the drill flank surface and the presence of aluminium chips on the drill bit's tip, the latter of which is the least adherent.

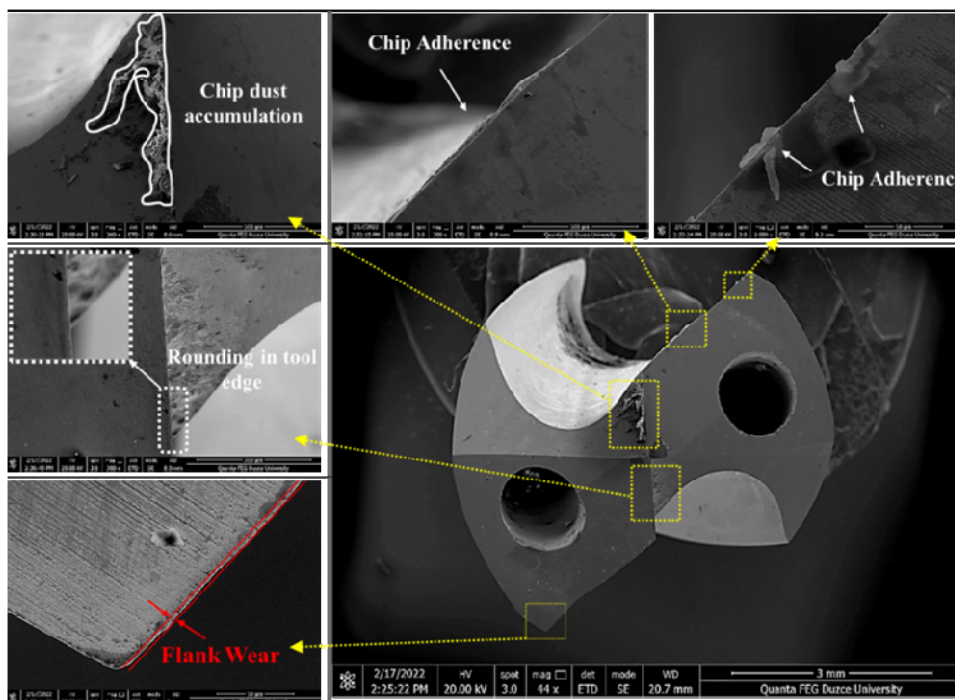


Figure 10. SEM morphology of the wear zones of drill Tool 1 after drilling CARALL composite.

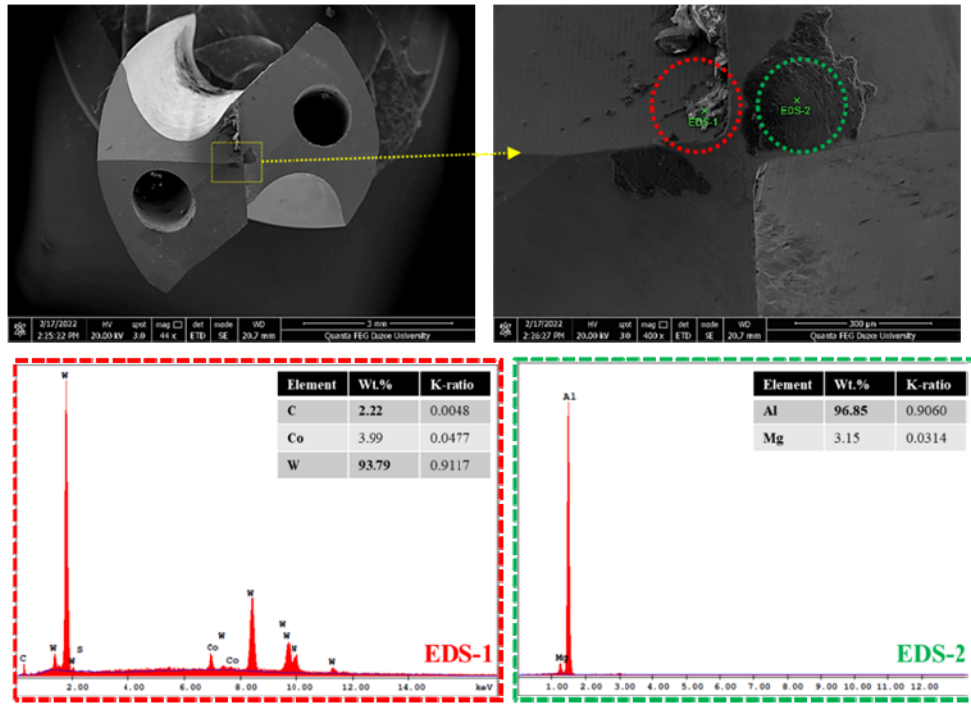


Figure 11. EDS evaluation of the elemental analysis of drill Tool 1 after drilling CARALL composite.

While Tool 2 shows severe abrasion wear and adhesion wear during the drilling of high-strength CARALL composite, Tool 1 does not show any wear. Figure 12 shows that a large region of powdery fibre dust around the drill chisel edge has been used to hold the drill in place. The collected chips after the drilling operation are analysed using energy-dispersive X-ray spectroscopy (EDS) to determine whether or not powdered carbon and aluminium chips are present in the accumulated chips (Figure 13). Furthermore, the flank wear and edge rounding caused by fibre abrasions are

revealed to be the most significant contributors to the wear development of the drill. The adhesion of fibre dust to the flank surface has also been observed, and edge chipping has been verified as the primary failure mechanism of this drill [28, 31]. This is due to the carbide's brittle nature, which makes it unable to withstand high stresses, resulting in chipping [43]. When it comes to Tool 1, the tool has the lowest capacity to withstand the intense wear that results from the high-strength CARALL drilling procedure, according to the results.

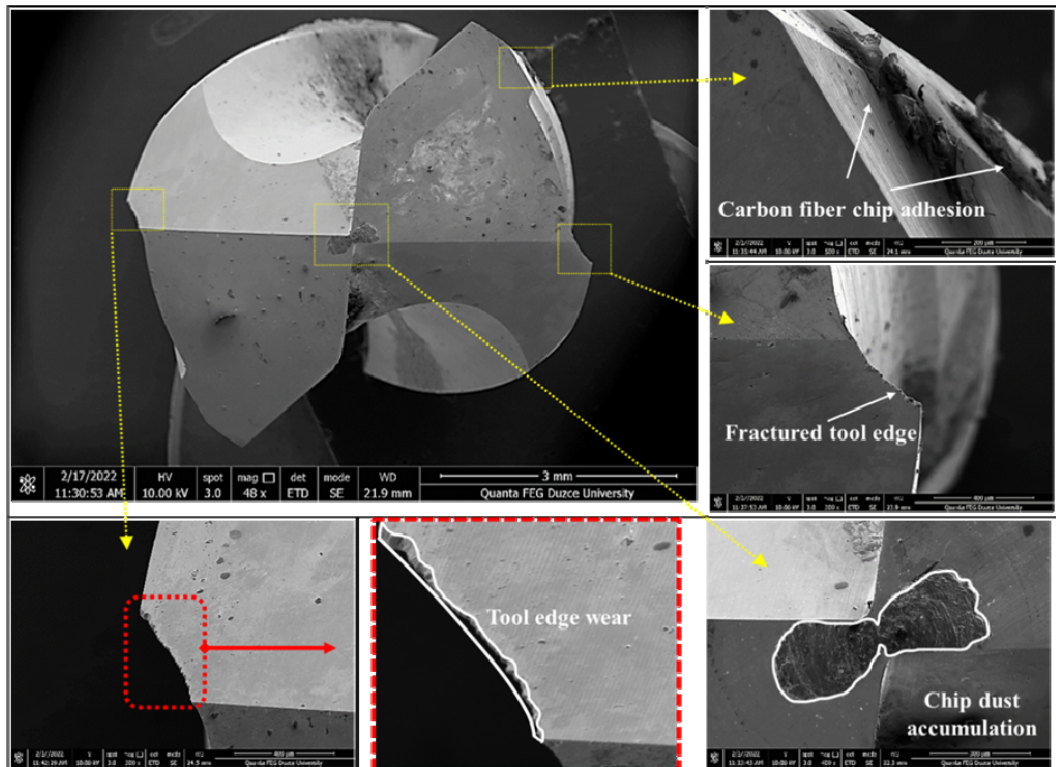


Figure 12. SEM morphology of the wear down surface of drill Tool 2 after drilling CARALL composite.

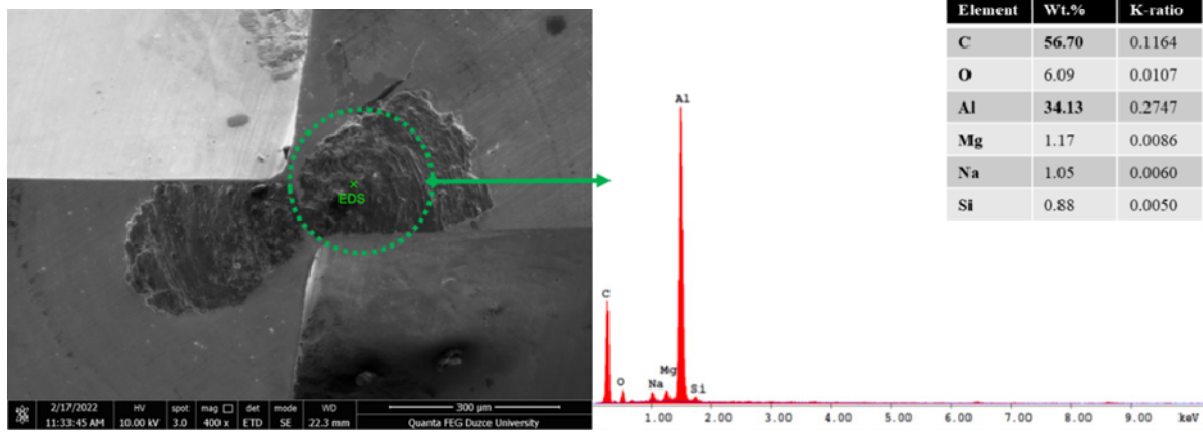


Figure 13. EDS evaluation of the elemental analysis of drill Tool 2 after drilling CARALL composite.

3.4 Statistical analysis of drilling characteristics

The study utilizes variance analysis (ANOVA) to ascertain the accuracy of the assumed experimental model. We perform the ANOVA test to statistically investigate the relevant machining output variables for Average thrust force (F_z), Average torque (T), and Surface roughness (S_a). The P-values for all the process variables present a significance level of 95%. Once the P-value (less than 0.05) has occurred and the R^2 converges to unity, the most significant variables for the output response value have been identified. This means the response model has been devised well and works better for further evaluation. Figure 14. a–c displays the Surface roughness (S_a), Average thrust force (F_z), and Average torque (T), i.e., a standardized probability plot; when the data is grouped on the near-fit line, it is evident that the data is relatively normal, with just

a tiny variation from the norm. There is no discernible pattern or uneven structure to it. The proposed model predictions are carried out under the desirable experimental quality required for cost-effectiveness and damage-free production.

The influence of altering characteristics on drilling responses for both tools has been studied for the CARALL composite's machining behaviour. As a result, a variable interaction-based regression model has been used to express the empirical regression model. Correlation analysis yields estimates of the experimental and prediction values' standard deviation. Figure 15. a–c shows that there is less discrepancy between the anticipated values and the measured surface roughness (S_a), Average thrust force (F_z), and Average torque (T).

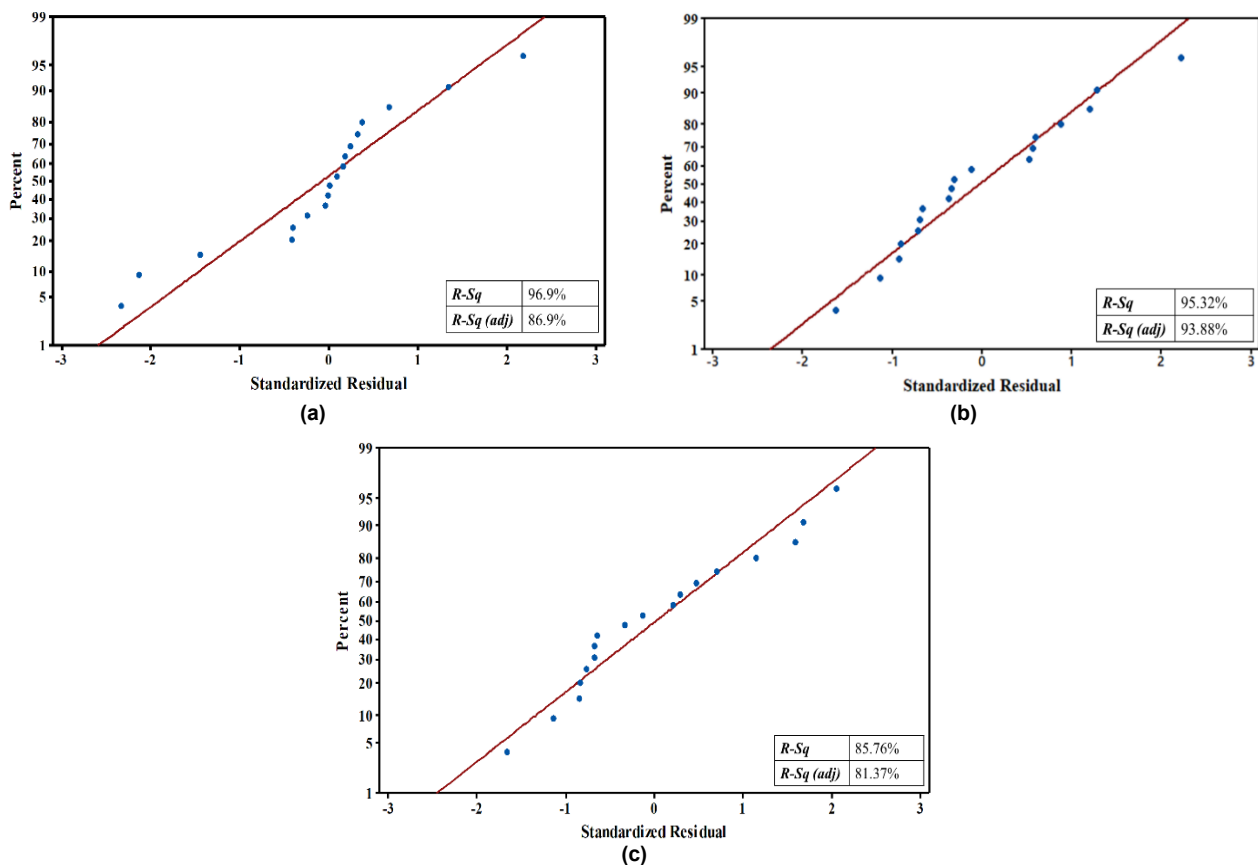


Figure 14. Normal probability plots for: (a) Surface roughness (S_a), (b) Average thrust force (F_z), and (c) Average torque (T).

The average error value is much lower, indicating the drilling test's viability. Tool 1 and 2 models are listed below for all three output parameters (Equations 10-15).

For Tool 1:

$$T = 29.6 + 0.062 \cdot Vc + 183.1 \cdot f - 1.219 \cdot Vc \cdot f \quad (10)$$

$$Fz = 45.6 + 0.145 \cdot Vc + 737 \cdot f - 2.14 \cdot Vc \cdot f \quad (11)$$

$$Sa = -0.28 + 0.0133 \cdot Vc + 7.6 \cdot f - 0.085 \cdot Vc \cdot f \quad (12)$$

For Tool 2:

$$T = 17.8 + 0.040 \cdot Vc + 243.2 \cdot f - 1.219 \cdot Vc \cdot f \quad (13)$$

$$Fz = 28.4 + 0.119 \cdot Vc + 808 \cdot f - 2.14 \cdot Vc \cdot f \quad (14)$$

$$Sa = -0.92 + 0.0321 \cdot Vc + 17.1 \cdot f - 0.085 \cdot Vc \cdot f \quad (15)$$

3.5 CoCoSo optimization method

The study employs the hybrid approach involving a blend of the Taguchi-based CoCoSo to identify the combination of the factors for achieving optimum machining performances. The second-order regression model developed by Taguchi's methodology is utilized to analyse Average torque (T), Average thrust force (Fz), and Surface roughness (Sa). The CoCoSo optimization method is applied to the three responses mentioned above for both tools individually, and optimal settings were obtained for Tool 1 and Tool 2 independently. The higher desired assessment score (K_{ci}) value in CoCoSo indicates the proposed MCDM optimization technique's effectiveness in improving the resulting element's manufacturing quality through higher yield. K_{ci} was computed by Equation 9 and illustrated in Table 4 for both tools.

Table 4. CoCoSo assessment score (K_{ci}) for both the tools.

Tool 1										
Exp. No.	Response Normalization			S_i	P_i	$w_i^0 = 1/3$				Rank
	Sa	Fz	T			H_{ci}	L_{ci}	M_{ci}	K_{ci}	
1	0.500	0.990	0.559	0.676	2.618	0.150	7.754	0.838	3.906	2
2	0.656	0.250	0.321	0.405	2.190	0.118	5.266	0.502	2.641	5
3	1.000	0.000	0.000	0.330	1.000	0.061	3.506	0.409	1.768	8
4	0.445	1.000	1.000	0.807	2.766	0.163	8.894	1.000	4.484	1
5	0.168	0.396	0.623	0.392	2.147	0.116	5.122	0.485	2.568	6
6	0.094	0.047	0.258	0.132	1.462	0.073	2.462	0.163	1.207	9
7	0.043	0.982	0.614	0.541	2.199	0.125	6.306	0.670	3.175	3
8	0.000	0.459	0.941	0.462	1.753	0.101	5.262	0.573	2.651	4
9	0.141	0.133	0.447	0.238	1.804	0.093	3.610	0.295	1.795	7
Tool 2										
1	1.000	0.920	0.778	0.890	2.893	0.163	7.747	1.000	4.051	1
2	0.158	0.489	0.397	0.344	2.071	0.104	4.091	0.387	2.075	6
3	0.655	0.000	0.000	0.216	0.870	0.047	2.074	0.243	1.074	9
4	0.415	1.000	0.852	0.748	2.696	0.148	6.814	0.840	3.548	2
5	0.246	0.531	0.596	0.453	2.284	0.118	4.877	0.509	2.499	4
6	0.000	0.142	0.468	0.201	1.303	0.065	2.499	0.226	1.262	8
7	0.299	0.973	1.000	0.750	2.662	0.147	6.785	0.842	3.535	3
8	0.107	0.558	0.518	0.390	2.108	0.108	4.363	0.439	2.227	5
9	0.237	0.223	0.492	0.314	2.023	0.101	3.887	0.353	1.964	7

Consequently, multifactorial aspects have come to be interpreted as a hybrid objective function for resolving the multi-attribute problem. As elaborated in this methodology, the assessment score is set to an assigned ranking order. Experiments 4 and 1 have been identified to possess the highest assessment score (highest aggregated single function) of 4.484 and 4.051 for Tool 1 and Tool 2, respectively. According to the CoCoSo assessment score (K_{ci}) obtained for the performed drilling experimentation, which indicates the optimum parametric setting as Cutting speed (Vc) – 70 m/min, Feed rate (f) – 0.08 for Tool 1, whereas Cutting speed (Vc) – 70 m/min, Feed rate (f) – 0.08 for Tool 2. It reveals that the elevated assessment score (K_{ci}) can be obtained between lower feed rate (f) and lower to moderate cutting speed (Vc) by both the drill bits.

3.6 Scanning Electron Microscopy (SEM) Test of The Machined Sample at Optimal Settings

While drilling CARALL composite, the sharp-edged and heated metal chips will likely cause substantial thermal deterioration and mechanical abrasion. The drilling of the CFRP layer to the aluminium layer is very susceptible to pyrolysis or glass transition temperature because of the heat-up drill bit flask that comes from machining earlier metallic layers [44]. Hence, inspecting the surface characteristics of drilled composite holes becomes more vital. Therefore, the assessments of the consequences of the drilling on CARALL composite at the optimal settings obtained from the CoCoSo MCDM technique for Tool 1 and Tools 2, respectively, have been evaluated to understand the effect of drilling on the surface of machined holes.

Figures 16 and 17 exhibit the SEM micrographs of characteristic surface morphological images of machined holes in CARALL composite to access the different drilling conditions using different drill bits and optimal cutting conditions, i.e., Tool 1 ($Vc = 91$ m/min and $f = 0.08$ mm/rev) and Tool 2 ($Vc = 70$ m/min and $f = 0.08$ mm/rev). The drilled hole in CARALL composite by Tool 1 displayed in Figure 16 shows a moderate degree of erosive wear to the CFRP layer surfaces due to the lower point angle of the drill bit, which reduces the influence of the aluminium chip ejection on the hole surfaces. Failure in composite layers occurs when a cutting force exerted by the drill bit surpasses the yield strength of composite layers, causing debris to be removed and holes or indentations to be left behind as the drill travels through the workpiece's intended surface [31, 45].

Figure 16 shows that interlaminar delamination, typified by a debonding failure between aluminium and adjacent carbon fibre layers, occurs virtually at the hole exit side due to the feed force pushing away the layers right beneath the drill tip being greater than the crucial thrust force [31]. To aggravate smearing, increasing cutting speed or reducing feed rate can lead to increased friction at the tool-workpiece interface or longer tool-workpiece contact time, which results in higher inter-face temperatures. This resin melt may have been exacerbated by the low heat conductivity of the CFRP layers used in CARALL composites. Due to the high pressures

and temperatures at the tool-workpiece interface, the redeposited materials on the cut composite surfaces seem mostly to be fibre dust or residual resin. Despite the unfavourable fibre cutting, there are few visible cavities or cracks [45]. While the SEM study divulges fragments comprising broken and bent fibres of CFRP layers adhering to the drilled composite holes randomly, matrix smearing is less existent for Tool 1 drilling cases. In other words, increasing the cutting speed or feed rate could increase thrust forces, which can impact the surface integrity of composite holes due to an increase in the area damaged by drilling. During drilling, highly heated drill flanks come into contact with the composite and cause thermal defects defined by fuzziness, pyrolysis, matrix softening, and degradation [31].

Comparatively, as seen in Figure 17, As a result of using Tool 2, Due to the inadequate ejection of aluminium chips, machining from CFRP to aluminium results in significant mechanical deterioration of the CFRP layers. CFRP surfaces are severely abraded by the sharp-edged metal chips that aggressively evacuate through the composite hole walls. The loss of matrix in the voids on the surface is primarily due to the mechanical erosion of metal chips. During drilling, heated aluminium chips could quickly coagulate at the machined hole surfaces, resulting in highly concentrated temperatures to CFRP layers with relatively limited thermal conductivity [46]. Due to the high temperatures, microcracks in the CFRP layers and softened matrix from the cut surfaces can be seen in Figure 17.

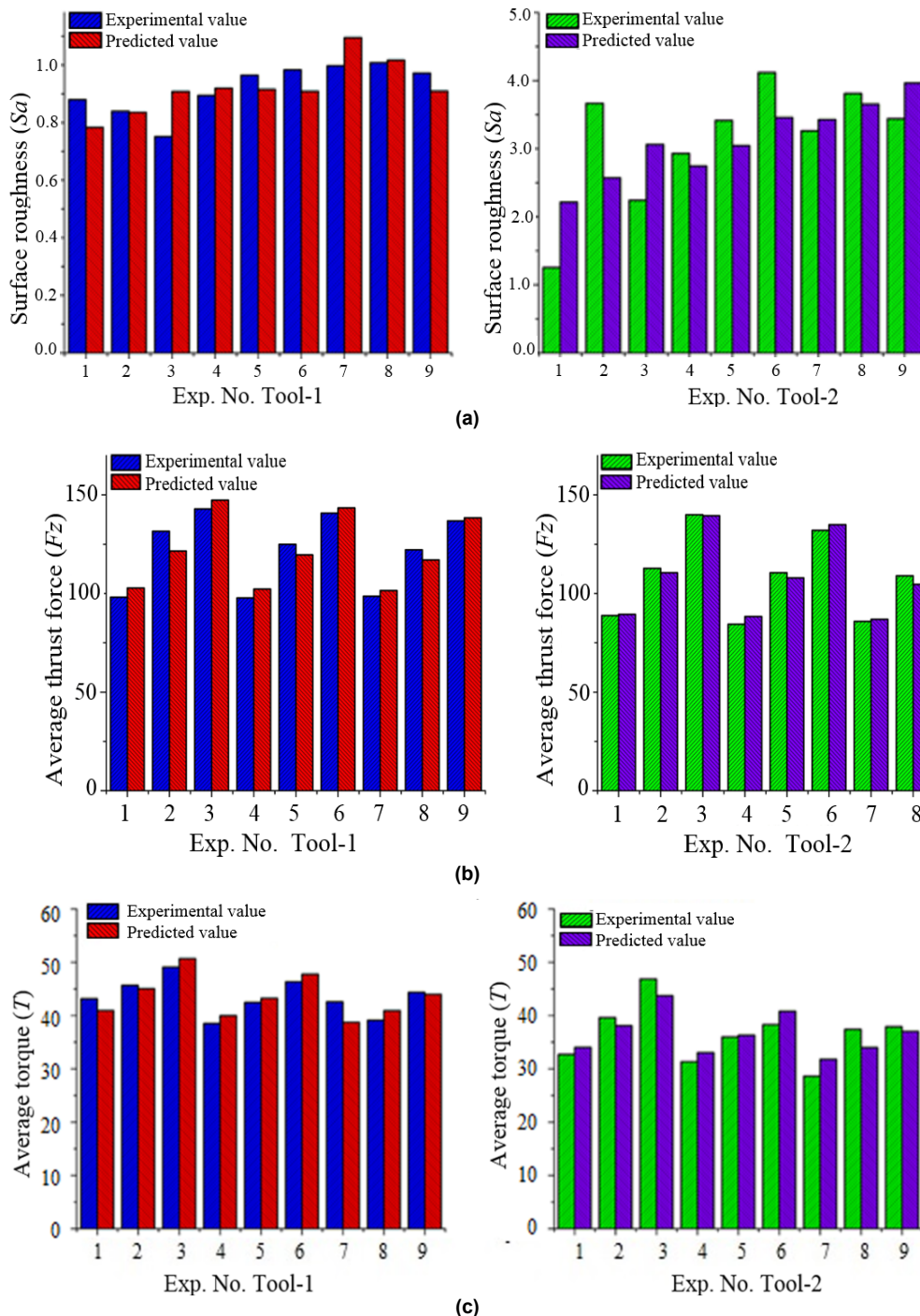


Figure 15. Comparison between experimental v/s. predicted values for: (a) Surface roughness (S_a), (b) Average thrust force (F_z) and, (c) Average torque (T)

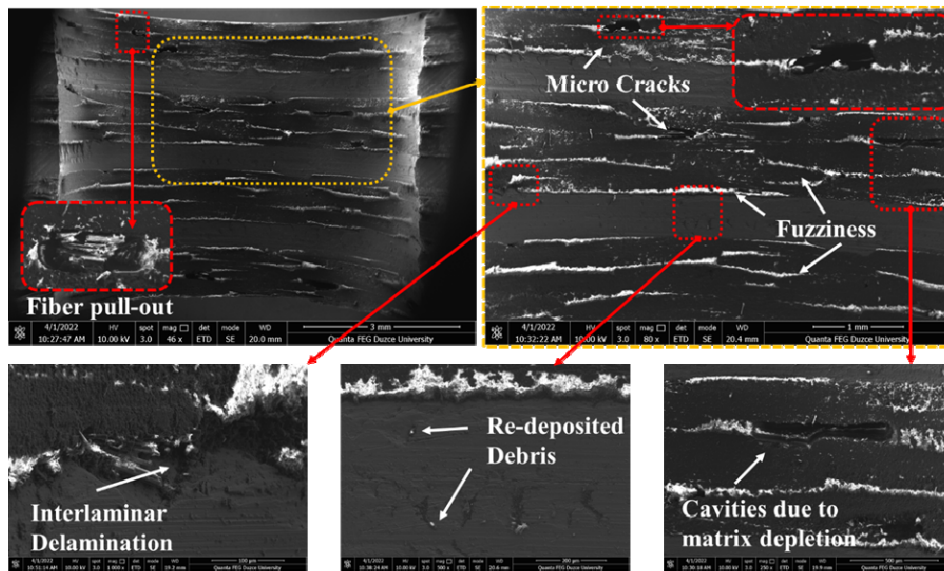


Figure 16. SEM morphologies of the CARALL composites holes produced by the Tool 1 at $V_c = 91$ m/min and $f = 0.08$ mm/rev.

The rough surface texture of CFRP is caused by the fractography of carbon fibres, caused by the bending of the fibres and the loss of the matrix. A substantial amount of damage, including microcracking, fibre fractures, adhesion, and fuzzing, could be seen on the machined CFRP hole surfaces. Interlaminar cracking is readily evident through SEM investigations of drilled holes. The unequal weight transmission across layers causes severe extrusion between adjacent plies [31, 42, 45]. The increased cutting temperatures with increasing

drilling depth cause considerable fibre debris and smearing composite matrix on the walls of the machined hole [47]. Magnified images of the hole morphologies reveal that the Tool 2 poorly cut surfaces were discovered during the examinations of the magnified views. Furthermore, the surface quality of the CFRP holes significantly deteriorates when drill bit geometry is changed, resulting in vast numbers of damaged or defective regions on the hole surfaces [48].

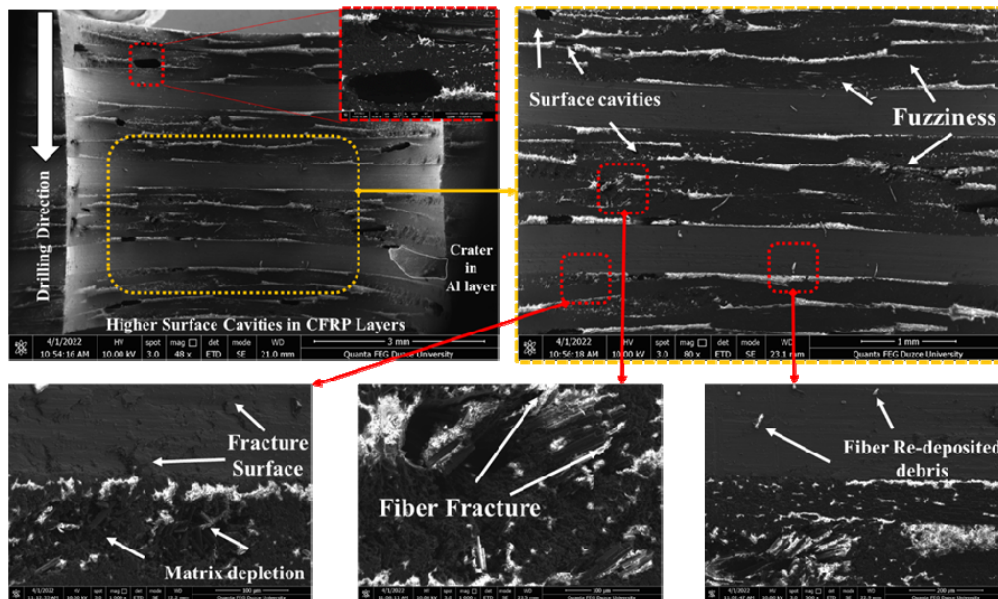


Figure 17. SEM morphologies of the CARALL composites holes produced by the Tool 2 at $V_c = 70$ m/min and $f = 0.08$ mm/rev.

4. CONCLUSIONS

The current article explores the machining aspect of stacked composite using two types of tool design. A metal alloy (Al5754) and a CFRP composite based on the CARALL composite represent aviation components. It is noted that the high-strength CARALL composite can be made more machinable by employing specific drills. Drilling forces, hole morphologies, and tool wear were accurately addressed concerning the

process parameters and the drill bits employed in the experiment. The following inferences and conclusions can be outlined based on obtained findings:

- For drilling CARALL composite, the results show many forms of thermal and mechanically induced damage to the hole wall surfaces, including interlaminar matrix smearing, cracking/cavities, and chip adhesion. Tool 2 achieved lower average thrust and torque results compared to Tool 1. In high-strength CARALL composite drilling, abrasive wear leads to drill edge roun-

ding, and adhesion wear results from powdery chip welding. In contrast, flank wear and edge chipping are the primary tool failure factors.

- The tool with the elevated chip flute length and a lower point angle performs well regarding drilling pressures, hole quality, and tool wear behaviour. Drilling high-strength CARALL composites damage-free requires a drill bit that is both functionally developed and a great fit between tool material and composite workpiece.

- The drilling responses were optimized using the CoCoSo technique. The obtained optimal settings for both tools were analysed and compared with the help of SEM morphology and 3D roughness profile.

- According to the findings, drilling CARALL composite damages the hole wall surfaces, including delamination of interlaminar layers. Also, the spreading of the matrix and the formation of cracks and cavities are critical causes during drilling operations. Drilling CARALL composite wear mechanisms include abrasive wear that causes drill bit edge rounding and adhesion wear caused by powdery chip adhesion.

- Analysis shows that Tool 1 has demonstrated the most effective and optimal drilled hole quality, machining forces, and tool wear. The results illustrate the necessity of optimizing machining parameters and the good fit between the tool material and the composite workpiece in attaining the damage-free drilling of hybrid composites like CARALL composite.

This study examines the impact of process constraints and machining assessment on CARALL composite by focusing on drilling responses, specifically drilling forces and hole quality. The results were explored by analysing different tool performances and exposing the tool wear modes. During the machining test, tool wear and hole quality significantly determine quality, productivity, and tool life. Delamination, temperature analysis, and the influence of drill bit material variation (uncoated and coated bits) are examples of the types of responses that might be evaluated in the future. The CARALL composite may be machined with various traditional (milling, turning, etc.) and non-conventional machining processes with the variation of stacking sequence and promoting production accuracy and variances. CARALL composite and other high-strength composites are used in various sectors, such as aircraft, vehicles, and home furnishings. Improvements can be made to several machining processes by correctly linking them to their corresponding process parameters.

ACKNOWLEDGMENT

The authors would like to sincerely thank the Çanakkale Onsekiz Mart University Scientific Research Projects Unit for supporting the project (No.FBA-2019-3170).

REFERENCES

- [1] Sadighi, M., Dariushi, S.: An experimental study of the fibre orientation and laminate sequencing effects on mechanical properties of GLARE, *Proc. Inst. Mech. Eng. G.J. Aerosp. Eng.*, Vol. 222, No. 7, pp. 1015-1024, 2008.
- [2] Liu, S., Sinke, J., Dransfeld, C.: An inter-ply friction model for thermoset based fibre metal laminate in a hot-pressing process, *Compos B: Eng.* Vol. 227, No. 7, pp. 1-14, 2021.
- [3] Wu, G., Yang, J.M.: The mechanical behavior of GLARE laminates for aircraft structures, *JOM: TMS*, Vol. 57, pp. 72-79, 2005.
- [4] Frizzell, R.M., McCarthy, C.T., McCarthy, M.A.: A comparative study of the pin-bearing responses of two glass-based fibre metal laminates, *Compos. Sci. Technol.* Vol. 68, No. 15-16, pp. 3314-3321, 2008.
- [5] Pranesh, R., Hemanathan, M., Babu, K. K., et al.: Mechanical characterization of glass fiber aluminium reinforced riveted joints, *FME Trans.*, Vol. 45, No. 1, pp. 89-92, 2017.
- [6] Purnowidodo, A., Iman, H.: Crack propagation behavior on metal laminate of FMLs after a high tensile overload under high constant amplitude load, *FME Trans.*, Vol. 48, No. 2, pp. 419-426, 2020.
- [7] Bellini, C., Cocco, V.D., Iacoviello, F., et al.: Performance evaluation of CFRP/Al fibre metal laminates with different structural characteristics, *Compos. Struct.* Vol. 225, pp. 1-10, 2019.
- [8] Botelho, E.C., Silva, R.A., Pardini, L.C., et al.: A Review on the development and properties of continuous fibre/epoxy/aluminum hybrid composites for aircraft structures, *Mater. Res.* Vol. 9, No. 3, pp. 247-256, 2006.
- [9] Vlot, A.: "Historical overview", Vlot A, Gunnink, J.W. (Eds.), *Fibre Metal Laminates: An Introduction*, Springer Dordrecht, pp. 3-21, 2001.
- [10] Che, D., Saxena, I., Han, P., et al.: Machining of carbon fibre reinforced plastics/polymers: A literature review, *J Manuf. Sci. Eng.* Vol. 136, No.3, pp. 1-22, 2014.
- [11] Giasin, K., Hodzic, A., Phadnis, V., et al.: Assessment of cutting forces and hole quality in drilling Al2024 aluminium alloy: experimental and finite element study, *Int. J. Adv. Manuf. Technol.*, Vol. 87, pp. 2041-2061, 2016.
- [12] VaziriSereshk, M.R., Bidhendi, H.M.: Evaluation of revealing and quantifying techniques available for drilling delamination in woven carbon fibre-reinforced composite laminates, *J Compos. Mater.* Vol. 50, No.10, pp. 1377-1385, 2016.
- [13] Hocheng, H., Tsao, C.C.: Effects of special drill bits on drilling-induced delamination of composite materials, *Int. J. Mach. Tools Manuf.* Vol.46, No. 12-13, pp. 1403-1416, 2006.
- [14] Khashaba, U.A.: Delamination in drilling GFR-thermoset composites, *Compos. Struct.* Vol.63, No.3-4, pp. 313-327, 2004.
- [15] Arul, S., Vijayaraghavan, L., Malhotra, S., et al.: The effect of vibratory drilling on hole quality in polymeric composites, *Int. J. Mach. Tools. Manuf.* Vol.46, No.3-4, pp. 252-259, 2006.
- [16] Abrão, A.M., Faria, P.E., Campos Rubio, J.C., et al.: Drilling of fibre reinforced plastics: A review, *J.*

- Mater. Process. Technol. Vol.186, No.1-3, pp. 1-7, 2007.
- [17] Brinksmeier, E., Janssen, R.: Drilling of multi-layer composite materials consisting of carbon fibre reinforced plastics (CRFP), titanium and aluminum alloys, CIRP. Ann. Manuf. Technol. Vol.51, No.1, pp. 87-90, 2002.
- [18] Giasin, K., Ayvar-Soberanis, S.: An Investigation of burrs, chip formation, hole size, circularity and delamination during drilling operation of GLARE using ANOVA, Compos. Struct. Vol.159, pp. 745–760, 2017.
- [19] Pawar, O.A., Gaikhe, Y.S., Tewari, A., et al.: Analysis of hole quality in drilling GLARE fibre metal laminates, Compos. Struct. Vol.123, pp. 350–365, 2015.
- [20] Park, S.Y., Choi, W.J., Choi, C.H., et al.: Effect of drilling parameters on hole quality and delamination of hybrid GLARE laminate, Compos. Struct. Vol.185, pp. 684–698, 2018.
- [21] Giasin, K.: The effect of drilling parameters, cooling technology, and fibre orientation on hole perpendicularity error in fibre metal laminates, Int. J. Adv. Manuf. Technol. Vol.97, pp. 4081–4099, 2018.
- [22] Giasin, K., Soberanis, S.A., Hodzic, A.: An experimental study on drilling of unidirectional GLARE fibre metal laminates, Compos. Struct. Vol.133, pp. 794–808, 2015.
- [23] Giasin, K., Gorey, G., Byrne, C., et al.: Effect of machining parameters and cutting tool coating on hole quality in dry drilling of fibre metal laminates, Compos. Struct. Vol.212, pp. 159–174, 2019.
- [24] Ekici, E., Motorcu, A.R., Yıldırım, E.: An experimental study on hole quality and different delamination approaches in the drilling of CARALL, a new FML composite, FME. Trans. Vol.49, No.4, pp. 950-961, 2021.
- [25] Ekici, E., Motorcu, A.R., Uzun, G.: Multi-objective optimization of process parameters for drilling fibre-metal laminate using a hybrid GRA-PCA approach, FME. Trans. Vol.49, No.2, pp. 356–366, 2021.
- [26] Liu, L., Qi, C., Wu, F.: Analysis of thrust force and delamination in drilling GFRP composites with candle stick drills, Int. J. Adv. Manuf. Technol. Vol.95, pp. 2585–2600, 2018.
- [27] Erturk, A.T., Vatansver, F., Yazar, E., et al.: Machining behavior of multiple layer polymer composite bearing with using different drill bits, Compos. Part B. Eng. Vol.176, pp.1-9, 2019.
- [28] Xu, J., An, Q., Chen, M.: A comparative evaluation of polycrystalline diamond drills in drilling high-strength T800S/250F CFRP, Compos. Struct. Vol.117, pp.71–82, 2014.
- [29] Zitoune, R., Krishnaraj, V., Almabouacif, B., et al.: Influence of machining parameters and new nano-coated tool on drilling performance of CFRP/Aluminium sandwich, Compos. Part B. Eng. Vol. 43, No. 3, pp. 1480–1488, 2012.
- [30] Koplev, A., Lystrup, A., Vorm, T.: The cutting process, chips, and cutting forces in machining CFRP, Composites. Vol. 14, No. 4, pp. 371–376, 1983.
- [31] Xu, J., Li, C., Chen, M., et al.: An investigation of drilling high-strength CFRP composites using specialized drills, Int. J. Adv. Manuf. Technol. Vol. 103, pp. 3425–3442, 2019.
- [32] Boughdiri, I., Giasin, K., Mabrouki, T., et al.: Effect of cutting parameters on thrust force, torque, hole quality and dust generation during drilling of GLARE 2B laminates, Compos. Struct. Vol. 261, pp. 1-16, 2021.
- [33] Marques, A.T., Durão, L.M., Magalhães, A.G., et al.: Delamination analysis of carbon fibre reinforced laminates: Evaluation of a special step drill, Compos. Sci. Technol. Vol. 69, No. 14, pp. 2376–2382, 2009.
- [34] Karpat Y, Deger B, Bahtiyar O. Drilling thick fabric woven CFRP laminates with double point angle drills, J. Mater. Process. Technol. Vol. 212, No. 10, pp. 2117–2127, 2012.
- [35] Devi, G.R., and Palanikumar, K.: Analysis on drilling of woven glass fibre reinforced aluminium sandwich laminates, Journal of Materials Research and Technology, Vol. 8, No. 1, pp. 1024–1035, 2019.
- [36] Xu, J., El Mansori, M.: Experimental study on drilling mechanisms and strategies of hybrid CFRP/Ti stacks, Compos. Struct. Vol.157, pp. 461–482, 2016.
- [37] Aamir, M., Tolouei-Rad, M., Giasin, K., et al.: Recent advances in drilling of carbon fibre-reinforced polymers for aerospace applications: A review, Int. J. Adv. Manuf. Technol. Vol.105, pp. 2289–2308, 2019.
- [38] Janakiraman, A., Pemmasani, S., Sheth, S., et al.: Experimental Investigation and parametric optimization on hole quality assessment during drilling of CFRP/GFRP/Al stacks, J. Inst. Eng. (India) Series C. Vol.101, pp. 291-302, 2020.
- [39] Kumar, D., Gururaja, S., Jawahir, I.S.: Machinability and surface integrity of adhesively bonded Ti/CFRP/Ti hybrid composite laminates under dry and cryogenic conditions, J. Manuf. Process. Vol.58, pp. 1075–1087, 2020.
- [40] Xu, J. et al.: Comparative study of minimum quantity lubrication and dry drilling of CFRP/titanium stacks using TiAlN and diamond coated drills, Compos. Struct. Vol.234, pp.1-13, 2020.
- [41] Liu, Y., Li, S., Li, H., et al.: The design and performance evaluation of assisted chip removal system in helical milling of CFRP/Ti stacks, Int. J. Adv. Manuf. Technol. Vol.108, pp.1297–1308, 2020.
- [42] Xu, J., El Mansori, M., Voisin, J., et al.: On the interpretation of drilling CFRP/Ti6Al4V stacks

using the orthogonal cutting method: Chip removal mode and subsurface damage formation, *J Manuf Process*. Vol.44, pp. 435–447, 2019.

- [43] Hrechuk, A., Johansson, D., Bushlya, V., et al.: Application of colding tool life equation on the drilling fibre reinforcement polymers, *Procedia. Manuf.* Vol.25, pp. 302–308, 2018.
- [44] Xu, J., Li, C., Chen, M., El Mansori, M. and Davim, J.P.: On the analysis of temperatures, surface morphologies and tool wear in drilling CFRP/Ti6Al4V stacks under different cutting sequence strategies, *Compos. Struct.* Vol. 234, pp.1-17, 2020.
- [45] Shao, Z., Jiang, X., Geng, D., et al.: The interface temperature and its influence on surface integrity in ultrasonic-assisted drilling of CFRP/Ti stacks, *Compos. Struct.* Vol. 234, pp.1-13, 2021.
- [46] Xu, J., El Mansori, M.: Numerical modeling of stacked composite CFRP/Ti machining under different cutting sequence strategies, *Int. J. Prec. Eng. Manuf.* Vol. 171, pp. 99–107, 2016.
- [47] Guo, C., He, J., Su, Y., et al.: Thermo-stamping curing process for CFRP/steel hybrid sheets and its interface strength improvement, *Compos. Struct.* Vol.241, pp. 1-28, 2020.
- [48] Geng, D., Liu, Y., Shao, Z., et al.: Delamination formation, evaluation and suppression during drilling of composite laminates: A review, *Compos. Struct.* Vol.216, pp. 168–186, 2019.

NOMENCLATURE

f	feed rate
h_x	local heat transfer coefficient
Fz	average thrust force
K_{ci}	assessment score
P_i	power weights
Sa	average surface roughness
S_i	weighted normalized matrix
T	average torque
$Tool$	cutting tool
Vc	cutting speed
w_i	weighted comparability

Abbreviations

Al	aluminium
ANOVA	variance analysis
ARALL	aramid-reinforced aluminium laminates
CARALL	carbon-reinforced aluminium laminates
CFRP	carbon-fibre reinforced polymer
CoCoSo	combined compromise solution analysis
DM	decision matrix
DoE	experimental design
EDS	energy-dispersive X-ray spectroscopy
FML	fibre metal laminate
GLARE	glass fibre aluminium reinforced epoxy
HNO ₃	nitric acid
MCDM	multiple-criteria decision-making
NaOH	sodium hydroxide
OA	orthogonal array
PCA	principal component analysis
SEM	scanning electron microscope

ПРОЦЕНА КАРАКТЕРИСТИКА ОБРАДЕ И ХАБАЊА АЛАТА ТОКОМ БУШЕЊА УГЉЕНИКА / АЛУМИНИЈУМ-АЛУМИНИЈУМ

**А.Р. Моторчу, Е. Екичи, С. Кесарвани,
Р.К. Верма**

У последњих неколико деценија, обрада влакана од ламината (ФМЛ) суочена је са критичним изазовима у контроли квалитета и надгледањем алата због унутрашње хетерогености и абразивности материјала. Различити алати за бушење коришћени су за истраживање ефекта параметара процеса на перформансе обраде. Композитне рупе и хабање алата проучавани су према сили бушења и хрупавости површине. Нагласак је био на испитивању морфологија алата и обухвата процесе који утичу на бушење CARALL композита. Одговори за бушење добијени за обе бушилице оптимизовани су коришћењем приступа одлучивању Виз; Комбинована анализа решења за компромисе (CoCoSo). СЕМ истрага обрађених узорака коришћена је за испитивање квалитета рупа и површинске завршне обраде. Бушилица под мањим углом са већом дужином бургије је дала најбоље резултате за бушење ЦАРАЛЛ композита, до одређеног нивоа са минималним бочним хабањем и адхезијом бургије.